Journal of Rehabilitation in Civil Engineering 13-3 (2025) 86-103

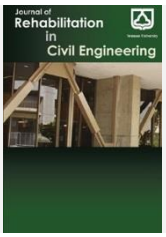

Journal of Rehabilitation in Civil Engineering

Journal homepage: https://civiljournal.semnan.ac.ir/

Durability of Rice Husk Ash Concrete in Chloride-Sulfate Environments

Nwzad Abduljabar Abdulla [1,*]

1. Professor, University of Salaheddin, Erbil, Iraq
* Corresponding author: *anwzad@yahoo.com*

ARTICLE INFO

Article history:
Received: 07 July 2024
Revised: 13 October 2024
Accepted: 03 November 2024

Keywords:
Chloride-sulfate environment;
Rice husk ash;
Sustainable concrete;
Strength;
Concrete permeability.

ABSTRACT

One of the challenges facing the construction industry is the durability of concrete in unfriendly environments. Cement substitute materials such as rice husk ash (RHA) can play a positive role in this direction. Therefore, the impact of rice husk ash on the behavior of concrete in an aggressive environment was examined experimentally by testing specimens partially submerged in solutions containing chloride and sulfate ions. The strength development and permeability of concrete mixes with 12% rice husk ash replaced by weight of cement were examined, in addition to normal concrete and concrete with a 5% superplasticizer (5%SP). The exposure duration and the maximum size of coarse aggregate were two of the test parameters. The outcomes of the experiments show that RHA enhances the properties of concrete and outperforms 5%SP and plain concrete. The compressive strength of RHA concrete was 40-60% higher than its equivalent plain concrete. After being exposed to the test solution for more than nine months, the 12%RH concrete's permeability was considerably lower than that of the other two types of concrete. A number of existing strength models were used to predict the splitting tensile and flexural strengths of RH concrete based on the compressive strength, yielding mostly conservative results.

E-ISSN: 2345-4423

How to cite this article: Abdulla, N. Abduljabar (2025). Durability of Rice Husk Ash Concrete in Chloride-Sulfate Environments. Journal of Rehabilitation in Civil Engineering, 13(3), 86-103. https://doi.org/10.22075/jrce.2024.34666.2133

1. Introduction

Concrete used in the construction of marine structures such as concrete bridges, retaining walls used in the construction of harbors, and off-shore concrete oil platforms is under the threat of physical damage and chemical changes that might lead to deterioration [1]. The splash zone is regarded as the most vulnerable part of a concrete structure to damage at sea. Chemical changes in concrete structures in the surge area and splash zone may lead to erosion [2]. Reinforced concrete structures in unsaturated concrete undergo deterioration in strength when subjected to a combined chloride and sulfate attack in aggressive environments. Ion diffusion, porosity variation, and water saturation of concrete are critical parameters for assessing the durability and service life of concrete structures [3]. Aggressive chloride and sulfate ions found in foundation soil, ground water, and seawater attack foundation concrete. This will substantially affect the durability of concrete in contact with saline soil environments, such as those in the southern parts of Iraq.

Products of cement hydration react chemically with sulfate ions in a number of ways. Because of the sulfate salts' recurrent crystallization, this may cause distress against the pore wall and cause surface scaling of concrete structures. Such distress has been observed in above-ground components of field structures [4]. The combined sulfate-chloride charge yields more strength loss and severe damage in concrete than when exposed to sulfate alone [5]. In the modern concrete world, material science is influenced by pozzolanic materials [6]. When added to concrete, mineral admixtures like rice husk ash increase the material's durability and sustainability. The agricultural residue, RHA, is a highly active pozzolanic material and is produced during the de-husking operation of paddy rice [7]. By mixing up to 30% of RHA with cement, it was possible to improve the strength and permeability of concrete without affecting their properties negatively [8]. Concrete containing RHA reduced the CO^2 emissions by 25% while increasing cost efficiency by 65% [9]. Permeability is the property that governs the rate of flow of a fluid through a porous solid. Penetration of materials in solution into the concrete may adversely affect its durability. This penetration depends on the permeability of the concrete, and since this determines the relative ease with which concrete can become saturated with water, permeability has an important bearing on the vulnerability of concrete to attack by aggressive solutions. Difference in circumferential and radial cracking expose the un-hydration products to water, this initiates the hydration process, leading to the self-sealing of the specimens. Blended concrete's permeability properties were substantially better than unblended ordinary concrete due to the addition of 30% reclaimed rice husk ash [8]. Concrete's strength and permeability are key attributes when operating in a hostile environment. This can be improved using cement replacement materials. However, very few studies have examined the long-term durability of concrete incorporating rice husk ash and exposed to chloride-sulfate solutions, which is the objective of present work. This is achieved by monitoring the performance of six different mixes of concrete. The compressive, splitting tensile, and flexural strengths development were observed for more than nine months. Furthermore, the permeability of the three types of concretes were scoped out.

2. Experimental program

2.1. Materials and mixing

Ordinary Portland cement was used as main binder for making the concrete. Rice husk ash was used for blending the Portland cement. The flow chart of the experimental work is depicted in Fig.1. The

chemical makeup of the cement, and rice husk ash is displayed in Table 1. The results of tests done to determine the physical characteristics of cement are displayed in Table 2. A 5% superplasticizer, by weight of water, was used in the mixtures (5%SP) and (12%RHA) to reduce the water demand. The river gravel was used as a coarse aggregate with two maximum sizes of aggregate; 10 and 20mm, respectively. The fine aggregate was quartzite sand with a fineness modulus of 1.5 and the grading fell into zone 3 of B.S. The rice husk was purchased from a nearby rice mill. It was grounded in a Los Angles machine, burned in an electric furnace, and then sieved [10]. The air permeability method was used to assess the fineness of RHA, as according to ASTM C204. After around 12 hours of grinding, a specific surface area of 26900 cm^2/g was obtained. The RHA utilized in this work can be categorized as an artificial pozzolan of siliceous material based on ASTM C618 criteria. Additionally, it satisfies the physical and chemical specifications of ASTM C618 class N pozzolan. On the day of mixing, both the sand and coarse aggregate (10 and 20mm maximum sizes) were thoroughly washed to remove dust as well as salts, and left in the open air to achieve the saturated surface dry condition.

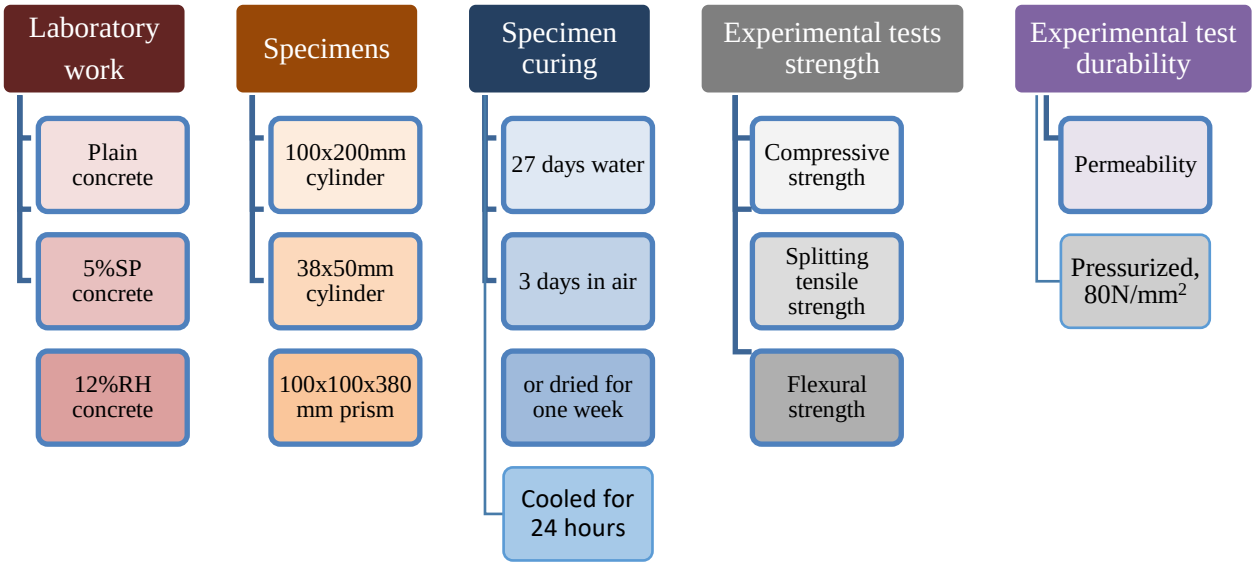

Fig. 1. Flow chart of the experimental Program.

The required quantity of RH ash was added to the cement, and then the materials were mixed dry by a trowel for a period of 10 minutes. Such a process was essential to breaking up the lumps or agglomerates of RH ash-powder particles and dispersing them throughout the cement particles.

Table 1. Chemical composition of cement, RHA.

Oxide (%)	Cement	RHA
CaO	62	1.5
SiO_2	22.8	86
Al_2O_3	4.2	2.6
Fe_2O_3	3.53	2.34
SO_3	2.06	1.72
MgO_4	3.28	1.44
Na_2O	0.32	0.43
K_2O	0.2	0.99
L.O. I	1.07	2.03
Ins. Residue	0.54	0.95

Table 2. Physical properties of cement.

Physical properties	Test results
Specific surface area Blaine method cm3/gm	3250
Specific gravity	3.15
Avg. particle size	15μm

For every maximum size of aggregate, three distinct concrete mixes were created: plain (P) concrete, melamine superplasticizer (5%SP) concrete, and twelve percent rice husk ash (12%RHA) concrete. All the concrete mixes were 1: 1.15: 1.3 (cement, sand, aggregate) and proportioned by weight for the six concretes. An acceptance criterion for fresh concrete tests is the slump test. For all the mixes, the w/c ratio was adjusted to give a constant workability of 90–100 mm slump in accordance with B.S. 1881, Part 2. This tolerance was necessary to achieve consistency among the concrete mixes and obtain a concrete with reasonable uniform quality. The use of RHA in concrete increases the water content of the mix due to the fineness of the RH. Melamine Superplasticizer was used to counteract the above effect and achieve the desired workability at a lower w/c ratio. The concrete mixtures were mixed in a revolving drum-type mixer with a capacity of $0.1m^3$ for 4 minutes. The cylindrical (100x200mm) and prismatic (100x100x380mm) specimens, intended for strength tests, were compacted on a vibrating table to ensure proper compaction, a minimum content of unwanted air, and maximum strength. For permeability tests, small concrete cylinders measuring 38 mm in diameter by 50 mm in depth were cast using coarse aggregate with a maximum size of 10mm. After casting, the specimens were covered with nylon sheets for 24 hours. After de-molding, the specimens were cured in water for 27 days, followed by 3 days in air.

2.2. Placing the specimens in the curing solution CI+SO

According to a report on underground water analysis of southern Iraq released by the Iraqi National Center for Geological Survey and Mines, the sulfate ion concentration ranges from 5000 to 7000 ppm, while the chloride ion concentration is between 20000 and 40000 ppm. For magnesium, the cation concentration falls between 1500 and 2000 ppm, for sodium, between 10,000 and 20,000 ppm, and for calcium, between 1000 and 1500 ppm. The concentrations of anions and cations in the curing solution used in this study were comparable to those found in contaminated soil and underground water in southern Iraq. The anions and salt concentrations were assessed based on the atomic weight of the element presents in the compounds, their molecular weight, and the chosen cation concentrations. The assumed cation concentrations for Na+, Ca++, and Mg++ were 2000 ppm, 1500 ppm, and 1750 ppm, respectively. The substances used to supply these ions were magnesium sulfate ($MgSO_4$) ($7H_2O$), calcium chloride ($CaCl_2.2H_2O$), and sodium chloride (NaCl). The above prepared test fluid was poured halfway into plastic containers containing the specimens 100x200mm cylinders, 100x100x380m prisms, and 38x50mm cylinders. Every ten days, the concentration of the solution was checked and adjusted so that half of thespecimens' depths were always submerged in the curing solution. The specimens were visually inspected before testing.

3. Experimental tests

3.1. Strength

To monitor strength development and strength reduction as a result of partially immersion in the test solution, cylindrical concrete samples (100*200mm) were tested to determine the compressive and

splitting tensile strengths. This size of cylinders was used in order to achieve fast saturation with the required test solution, Fig.(2a). Three cylinders were tested under compression load for each mix at the ages of 1, 2, 3, 6, and 9 months. Three cylinders were also used to check the changes in tensile splitting strength. For evaluating the flexural strength, two prismatic concrete samples (100* 100*380 mm) were tested under a three-point load at predetermined intervals in a similar manner to those of cylinders. In addition, compression tests were carried out at 1, 2, 3, and days just after 90 exposures.

3.2. Permeability

The term permeability normally relates to the ease with which a fluid will pass through a material under a pressure gradient but is also used to describe capillary, diffusion, adsorption, and absorption processes. The permeability test was carried out on small concrete cylinders measuring 38 mm in diameter by 50 mm in depth, Fig. (2b). Since the specimens were relatively small, the maximum aggregate size was limited to 10mm. All the small cylinders were exposed to identical environmental conditions, partially submerged in concrete CI+SO solutions, for a period of 9 months, Fig. (2a). The permeability tests were performed on days 1, 2, 3, and 4, immediately following 9 months exposure. The testing apparatus consists of two parts, mainly the permeating liquid accumulator and the specimen holder, Fig. (3a). In addition, an air compressor was used to inject the aggressive solution, maintained in the solution accumulator, into the test specimen, as shown schematically in Fig. (3b). The specimens were oven dried for one week, cooled for 24 hours, and then placed in the pressure vessel to accelerate the saturation process. Using the same aggressive solution, the specimen was subjected to a pressure of 3.5 N/mm^2 for a period of one week. Afterwards, the testing sample was inserted into the core holder. Compressed air was used to pressurize the specimen to 60 N/mm^2, and the average rate of flow was measured every 24 hours until there were no further changes in the rate of flow. The three types of concrete specimens were tested at 90 days under a pressure of 60 N/mm^2 did not exhibit any outflow. To allow differentiation in flow between various types of concrete, the driven pressure was increased to the maximum allowable value, i.e., 80 N/mm^2, and maintained for 4 days. At the age of 90 days, the average rate of flow was recorded daily until there was no further change in the flow rate.

Fig. 2. Cylinders: (a) (100x200mm); (b) (38mm x 50mm) partially submerged in the curing mixture.

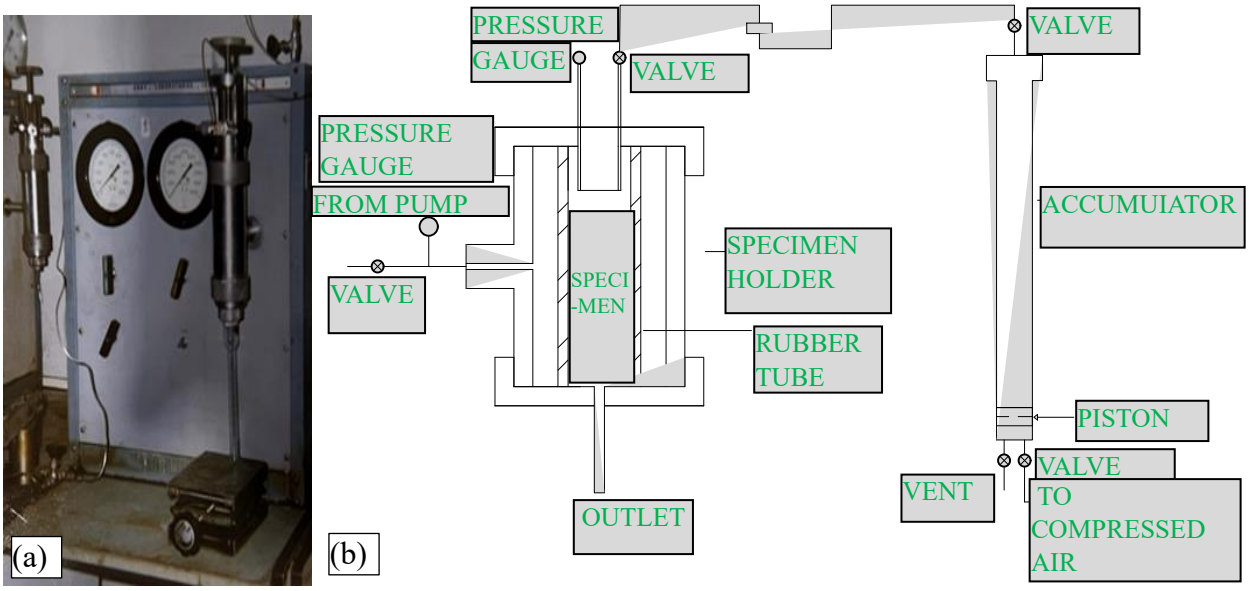

Fig. 3. Permeability testing apparatus: (a) actual; (b) schematic.

The measured flow rates were used to calculate the coefficient of permeability using Darcy's equation for flow through porous media:

$$\frac{d_Q}{d_T}\frac{1}{A_c}=K_p\frac{dH}{L} \quad (1)$$

Where: rate of flow through sample (cm^3/sec) = $\frac{d_Q}{d_T}$; change in hydraulic head across sample (cm)= dH; thickness of specimen (cm)= L=; the cross-sectional area of the specimen subjected to the fluid (cm^2) = A_c; permeability coefficient (cm/sec) = K_p.

4. Test results and discussions

The composition solution was intended to simulate realistic aggressive attacks on foundations in contact with soil. Such real conditions exist in regions near the sea, in harbor soil and in some aggressive environments. Concrete deterioration is usually exacerbated by sulfate attacks. Concrete in a non-aggressive environment is a sound, strong and long-living building material.

4.1. Strength

4.1.1. Compressive strength

Differential curing across members will affect the longer-term hydration resulting in temperature difference between exposed and submerged parts of the concrete. This will yield strength differences among the same members. The variations in the compressive strength for the duration of the test for plain and blended concretes with a maximum aggregate size of 10mm is presented in Fig. (4a), for different durations of exposure to $Cl^-+SO_4^{--}$ solution. The same strength development for concrete with a maximum aggregate size of 20mm is shown in Fig. (4b). The strength development for plain concrete continued for up to 6 months. Thereafter, there was a slight reduction in strength. The reduction in strength was due to decomposition and leaching out (CaO dissolves) as a result of attack by the sulfates and chlorides in the test solution [1]. The plain concrete performance was inferior to concrete containing only superplasticizer (SP). The SP is a very high molecular weight polymer, with a size 10000 to 100000 times that of a water molecule, which reduces bleeding and segregation of

fresh concrete [11]. Superplasticizers break up floes of cement particles. This releases water that improves workability and provides for better access of water to the cement particles, which results in a greater degree of hydration and higher strength. It can be seen that the 5%SP performed better than the plain concrete without SP. The strength increase appears to be related to a decrease in the courser porosity of the cement-silica fine paste system [12]. The superior performance of RHA is attributed to its high pozzolanic activity. Furthermore, RHA results in the partial obstructing of the voids and pores, leading to a reduction in pore size and a lower effective diffusivity for chloride [12].

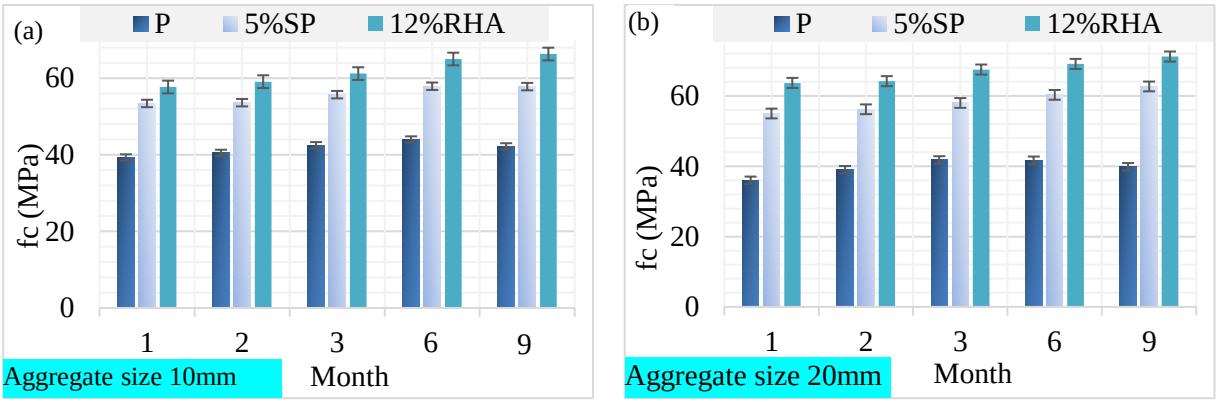

Fig. 4. Compressive strength versus curing period for plain and blended concretes with.

maximum size of coarse aggregate equal to: (a) 10mm; (b) 20mm.

4.1.2. Tensile splitting strength

Tensile splitting strength versus duration period in aggressive solution is plotted in Fig. 5 for different concretes with maximum aggregate size of 10 and 20mm, respectively. It can be seen that splitting strength changes similarly to that of compressive strength, Fig. 4. The improvement in tension and split strength of blended concrete is due to the better resistance of this concrete to the penetration and ingress of aggressive ions and impurity particles which tend to attack the internal cement matrix and reduce the strength of concrete [11]. In general, the tested specimens behaved better in compression than in tension.

4.1.3. Tensile splitting strength-compressive strength relationship

The relationship between splitting tensile strength and compressive strength of all concretes with maximum aggregate size of 10mm and 20mm is depicted in Fig. 6.

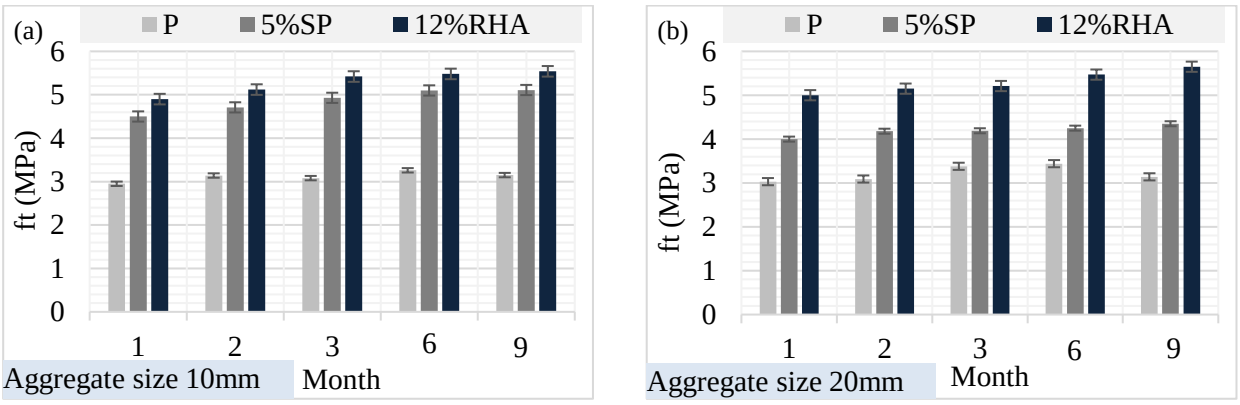

Fig. 5. Tensile splitting strength versus curing period for plain and blended concretes with: (a) 10mm; (b) 20mm maximum size of coarse aggregate.

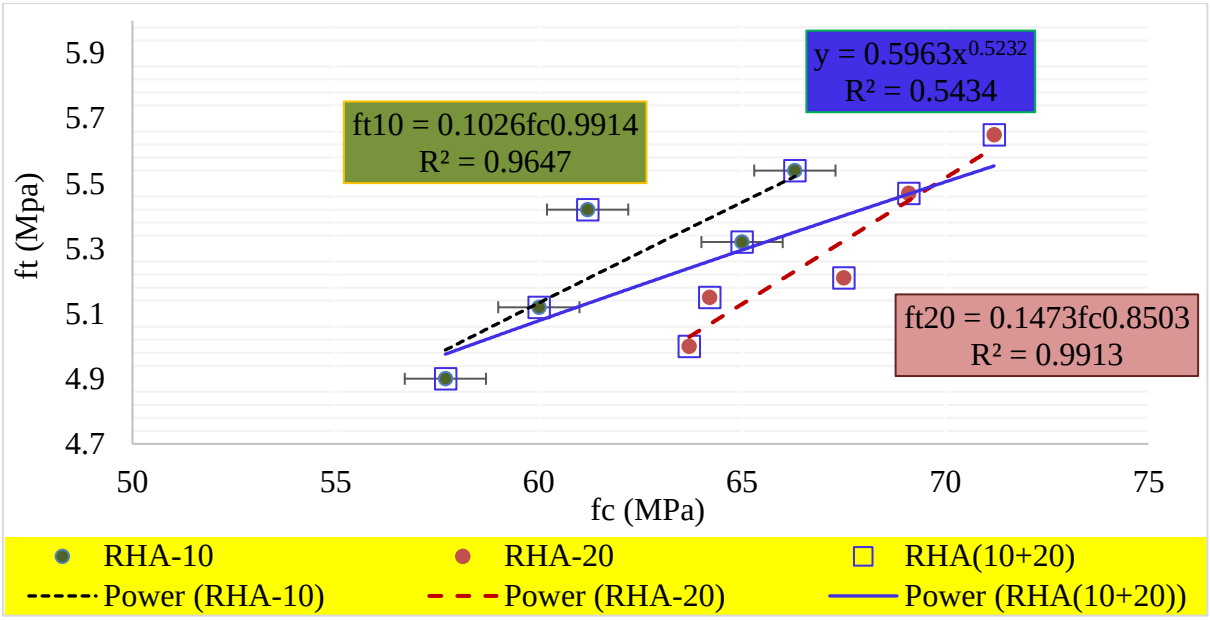

Fig. 6. Tensile splitting strength versus compressive strength for specimens with 12%RHA, maximum aggregate size of 10, and 20mm.

It is evident that when compressive strength rises, splitting tensile strength also increments. The relationship between concrete's tensile splitting strength and compressive strength has been the subject of numerous investigations. Several standard codes and individual studies proposed models for predicting the tensile splitting strength based on compressive strength. A number of standard models, Eqs. 2 to 4 were proposed by EC-04 [13], JCI-08 [14], ACI 318–11 [15] are shown below:

$$f_t=0.3f_c^{\frac{2}{3}} \quad (2)$$

$$f_t=0.13f_c^{0.85} \quad (3)$$

$$f_t=0.53f_c^{0.5} \quad (4)$$

Models put out by separate studies are also displayed here (Eqs. 5 to 9): Oluokun [16], Smadi and Migdady [17], Gesoglu et al. [18], Babua et al. [19], Meraz et al. [20]:

$$f_t=0.2f_c^{0.7} \quad (5)$$

$$f_t=0.46f_c^{0.5} \quad (6)$$

$$f_t=0.27f_{cu}^{\frac{2}{3}} \quad (7)$$

$$f_t=0.358f_{cu}^{0.675} \quad (8)$$

$$f_t=0.039f_c^{1.21} \quad (9)$$

From the regression analysis of the preset study experimental results, the following models is developed for RHA-concrete, Fig. 6:

$$f_t=0.596f_c^{0.52} \tag{10}$$

In Figs. 7 and 8, the predictions made by individual research and standard codes, Eqs. 2 to 9, were plotted against the experimental findings.

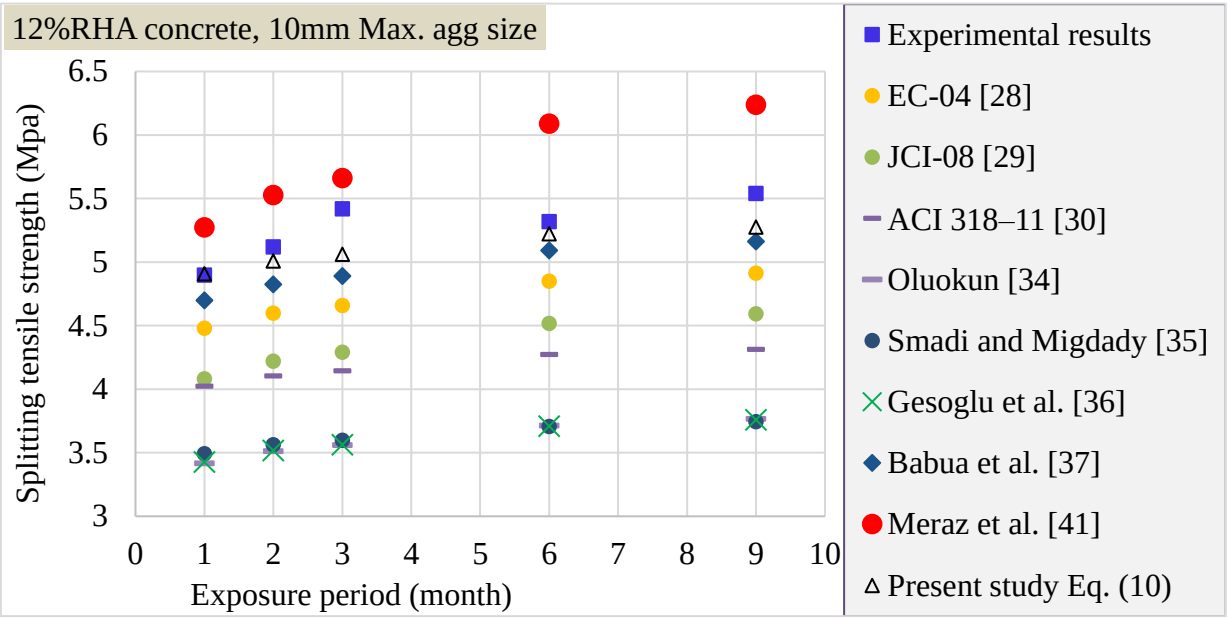

Fig. 7. Predicted and experimental tensile splitting strength of 12% RHA specimens, Max. agg. Size=10mm.

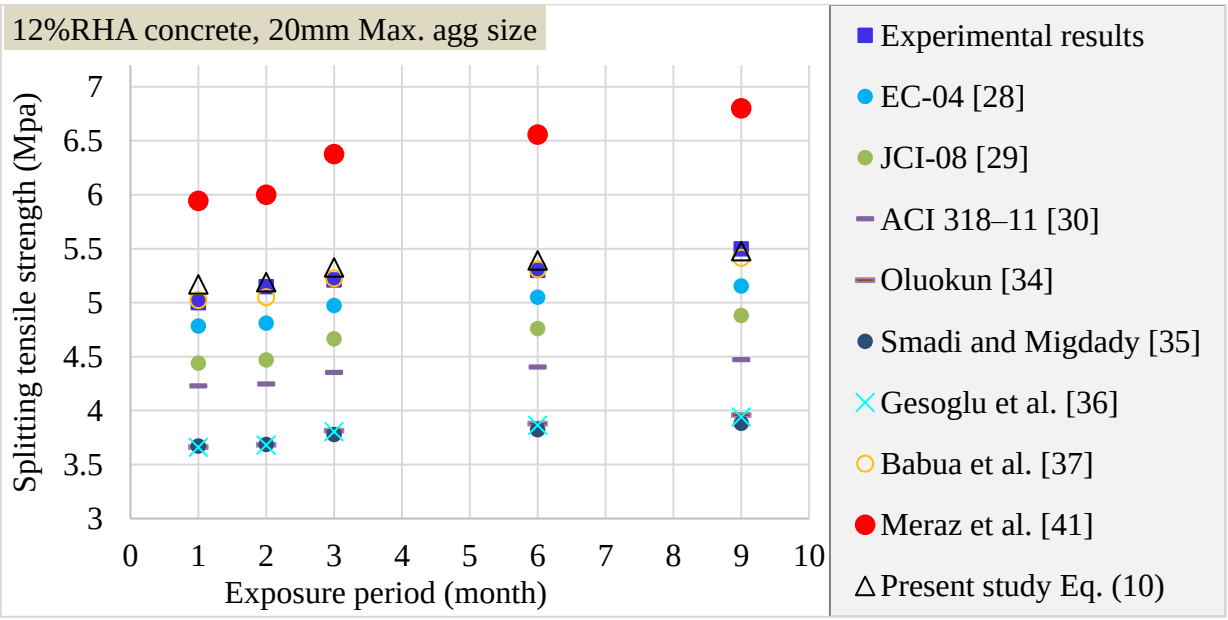

Fig. 8. Predicted and experimental tensile splitting strength of 12% RHA specimens, Max. agg. Size=20mm.

The proposed model predictions, Eq. (10), are also displayed in Figs. 7 and 8 for 12%RHA specimens with maximum aggregate size of 10, and 20mm, respectively. Comparing the models given in Eqs. (2) to (9) and the proposed model, it is evident that the Eq. (8) predict the experimental results more accurately.

4.1.4. Flexural strength

The variation in 1, 2-, 3-, 6-, and 9-months' flexural strength of plain and blended concretes are shown in Fig. 9. The flexural strength varied in the same way as compressive strength. As stated earlier, the weaker performance in tension compared to compression may be due to micro-cracking in the interfacial transition zone, which has a more damaging effect on flexural strength than on compressive strength of concrete. The boundary aggregates in cement create a wall-effect. This explains the greater porosity and the concentration of portlandite crystals and of ettringite in the transition zone [12].

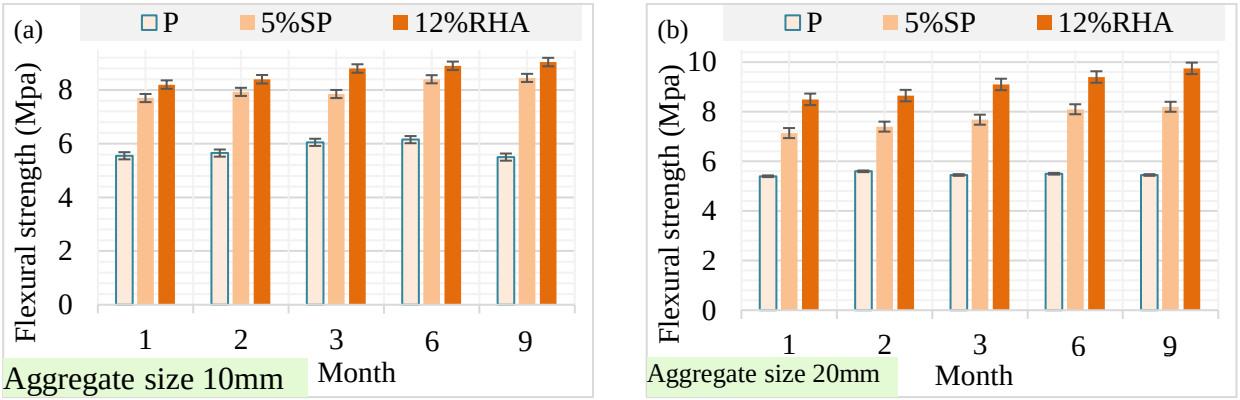

Fig. 9. Flexural strength versus curing period for plain and blended concretes with: (a) 10mm; (b) 20mm maximum size of coarse aggregate.

4.1.5. Flexural strength-compressive strength relationship

Models for predicting the flexural strength based on compressive strength were presented by a number of standard codes and independent investigations. The following standard models, Eqs. (11) to (13), were recommended by EN-1992-1-1 [13], ACI-318 [15], A 3600–2018 [21]:

$$f_r=0.435f_c^{\frac{2}{3}} \tag{11}$$

$$f_r=0.62f_c^{0.5} \tag{12}$$

$$f_r=0.6f_c^{0.5} \tag{13}$$

And another study, Meraz et al., [20] proposed the following model:

$$f_r=0.37f_c^{0.8} \tag{14}$$

The following model is used to predict the flexural strength of concrete based on its compressive strength, derived from regression analysis of the experimental results for RHA concrete (Fig. 10):

$$f_r=0.376f_c^{0.76} \tag{15}$$

Using the model developed in this study, Eq. (15) the anticipated and experimental values of flexural strength, the relationship between them is shown in Figs. 11 and 12 for 12%RHA specimens with maximum aggregate sizes of 10, and 30mm, respectively. Out of all the equations in Figs. 12 and 13, the predictions made by the proposed model, Eq. (15), produce more accurate results.

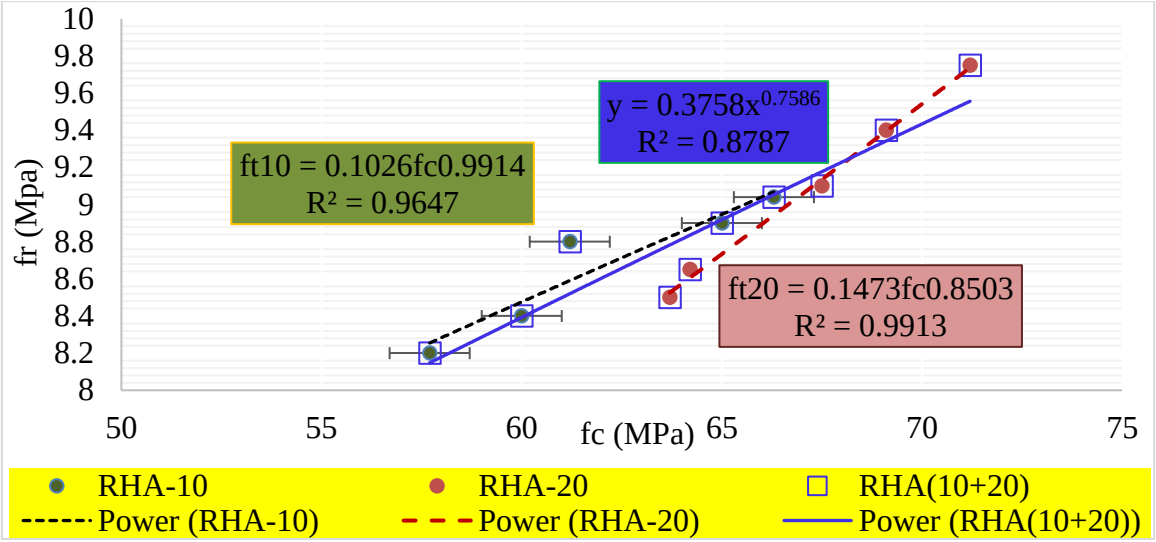

Fig. 10. Flexural strength versus compressive strength for specimens with 12%RHA.

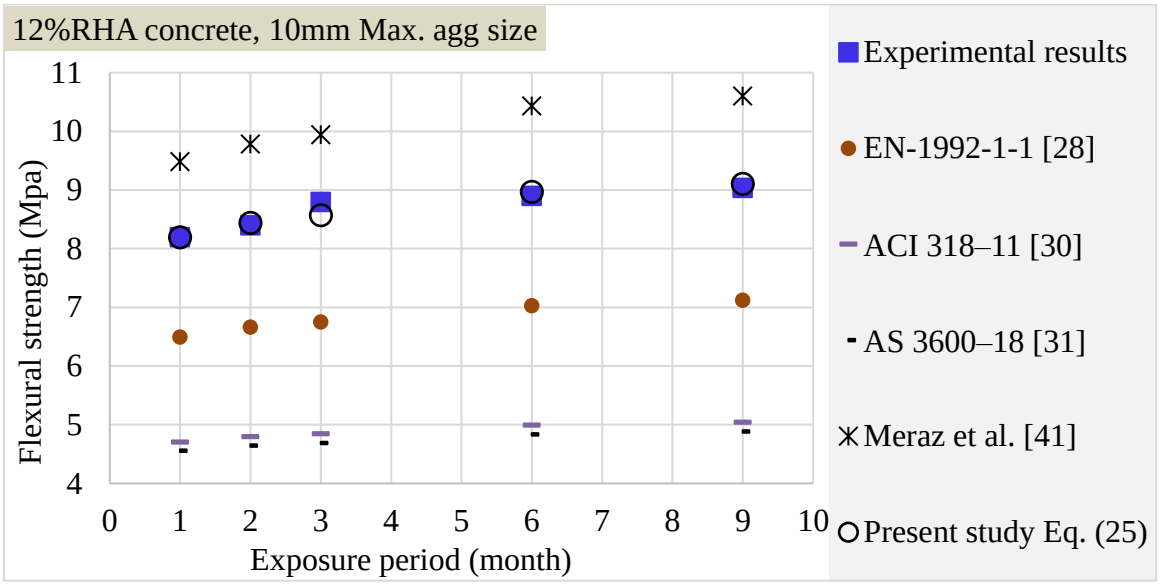

Fig. 11. Predicted and experimental flexural strength of 12% RHA specimens, Max. agg. Size=10mm.

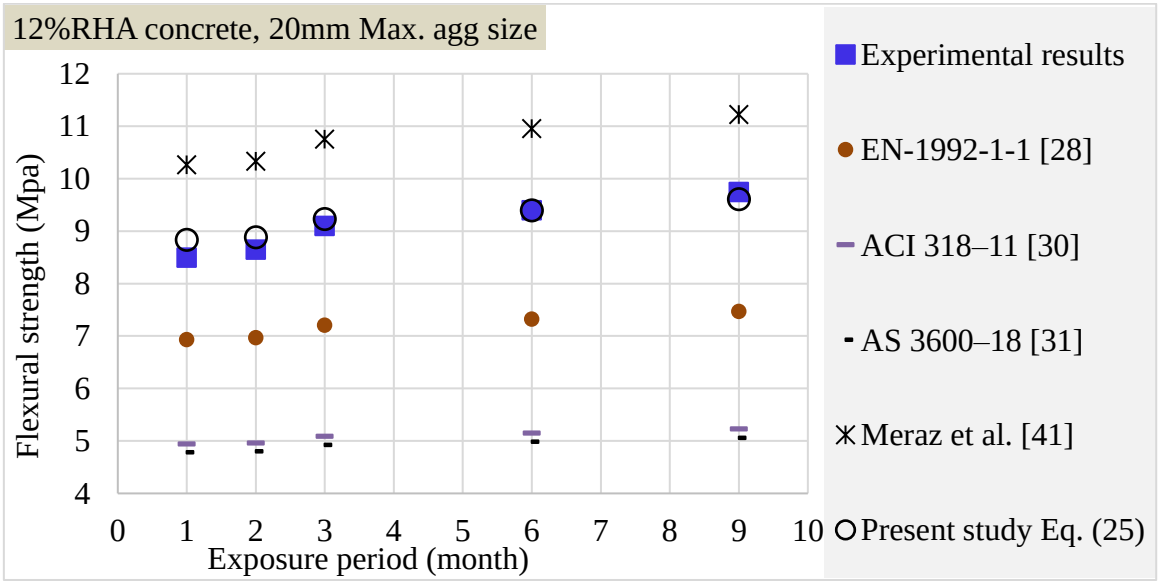

Fig. 12. Predicted and experimental flexural strength of 12% RHA specimens, Max. agg. Size=20mm.

4.1.6. 3D scatter plot

The relationship between the variables ft and fc, and ft and fr are shown in Figs.13 (a) and (b), respectively, for exposure periods of 1,2, 6, and 9 months. The same relationships for concrete incorporating RH are shown in Figs. 14 (a) and (b), where more uniform results are observed for the latter type of concrete.

4.2. Effect of maximum size of aggregate

For plain and superplasticizer concretes, the specimens with 10 mm maximum size coarse aggregate showed better compressive strength performance than the specimens with 20mm maximum size coarse aggregate, Fig.4. This is ascribed to the elimination of cracking in cement paste that encapsulates the coarser aggregate particles. But this trend was not observed in blended concretes with 10 and 20 mm maximum-sized coarse aggregate. This was due to the increase in the surface area of the 10mm coarse aggregate particles compared with 20mm particles, as both concrete mixes with 10mm and 20mm were designed for the same workability. This resulted in a partial reduction in water demand for the concrete mixes with 20mm maximum size of aggregate. Therefore, a lower w/c ratio and higher SP dosage was associated with concrete having 20mm maximum size of aggregate. The above trend was also observed in specimens tested for tensile splitting strength and flexural strength, Figs. 7 and 11. Although the strength of laboratory concrete will be different from site concrete due to better control, casting compaction and curing of the first one, its hoped that the laboratory results will give a good guide about the actual conditions that exist in the real structure. Pozzolanic materials have positive effect on the rheological properties of concrete [22]. Thus, Complementary component such as silica fume have a fundamental role in improving the mechanical properties of concrete [23].

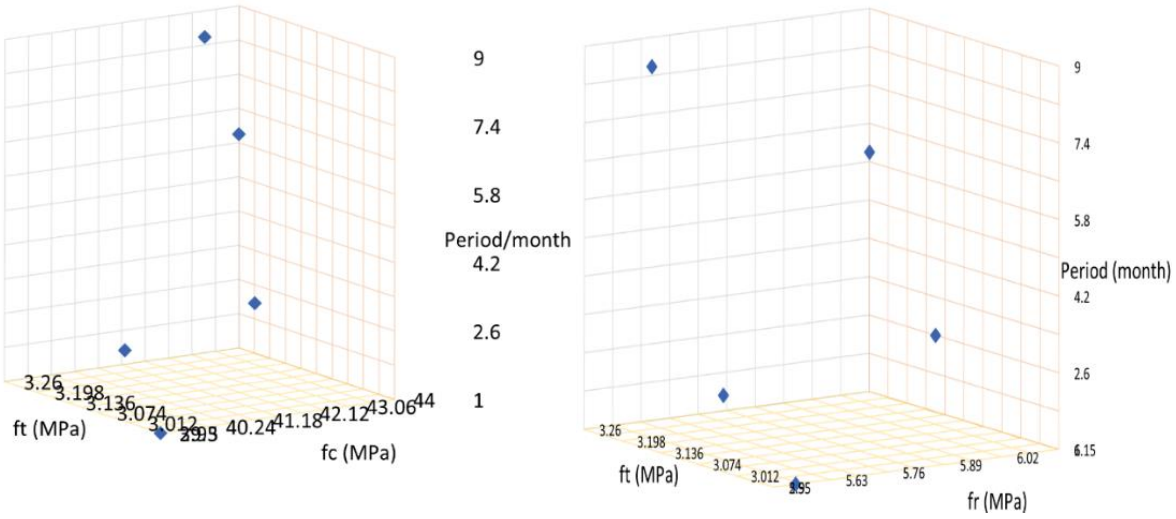

Fig. 13. Three D scatter plot: (a) ft-fc vs period; (b) ft-fr vs period for plain concrete with 10mm maximum aggregate size.

Generally, the strength development was continuous and improved during the first six months of exposure to the solution. However, in the last three months of exposure, the strength development slowed down and stopped in the case of plain concrete. The wide variation in the performance of blending materials may be attributed to the variation in the physical, chemical and mineralogical composition. This result from the industrial process related to their production and from the properties of the raw materials used [24].

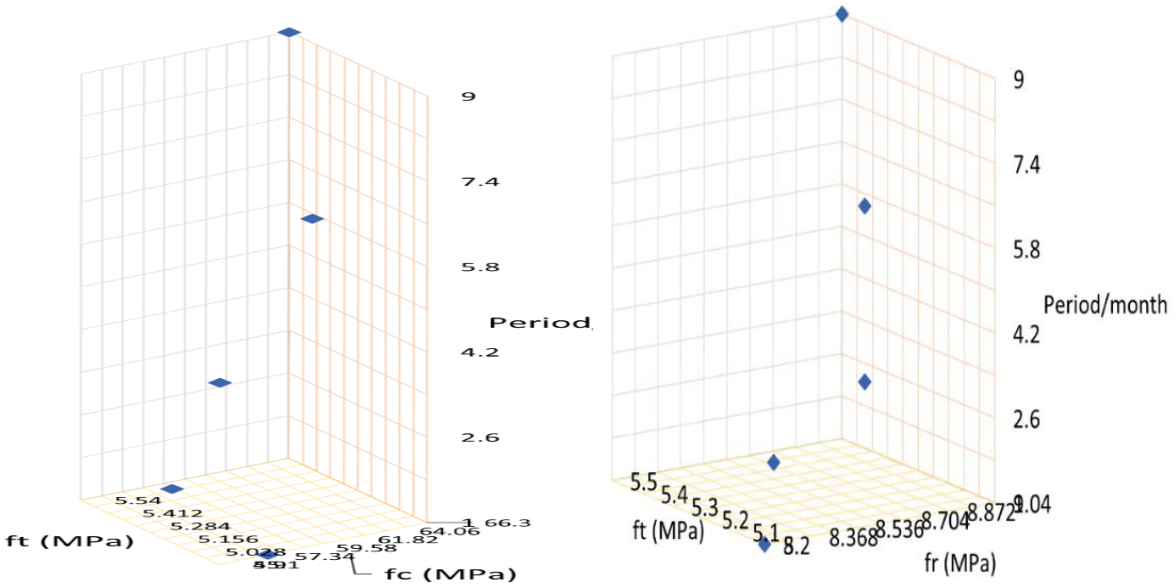

Fig. 14. Three D scatter plot: (a) ft-fc vs period; (b) ft-fr vs period for 12%RHA concrete with 10mm maximum aggregate size.

4.2.1. Contour plot

The relationship between two independent variables ft and fr and a dependent variable fc is shown in Fig. 15 (a) for P concrete with maximum aggregate size of 10mm. The equivalent figure for 12%RHA is depicted in Fig. 15(b). The contour lines and bands demonstrate the fc value in each case. The change in contour of lines and bands illustrate change in the strength value.

4.3. Permeability

For concrete materials facing the challenge of aggressive environments, it's important to evaluate their long-term durability and performance. The coefficient of permeability-duration test relationship for reference and blended concrete specimens with maximum aggregate sizes of 10 were dependent on the type of concrete. For the given maximum aggregate size and duration of the test, the blended concretes showed significant reduction in coefficient of permeability compared with their reference concretes. When concrete specimens exposed to drying and re-saturating, reductions in permeability encountered, self-sealing of concrete, the permeabilities of all tested concretes reduced with the curing age [25].

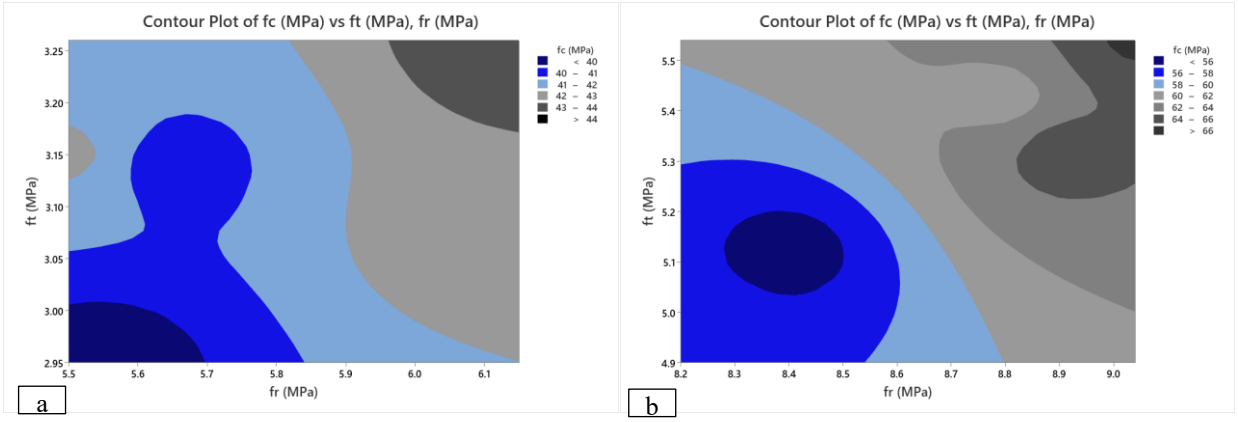

Fig. 15. Contour plot of fc vs ft, fr: (a) plain concrete; (b) 12%RHA concrete with Max. agg. Size of 10mm.

The heterogeneous microstructure of concrete plays a significant role in affecting the permeable qualities of concrete [25]. The coefficient of permeability indicates different values for various types of concrete, and decreased in the following order: plain concrete, 5%SP concrete, and 12%RHA concrete. The high performance of 12%RHA concrete compared to 5%SP concrete and plain concrete may be associated with the effect of the highly active pozzolans on the transition zone. The primary decrease in permeability happens in the first 24 hours and stays generally constant after 100 hours of testing [24]. The comparison of the rates of reduction in permeability due to blending materials shows that the rates are different from plain concrete. The progress of hydration leads to a decrease in permeability, which is further reduced in the presence of RHA due to the pozzolanic activity [24].

4.4. Compressive strength-permeability relationship

In Fig. 16, the results of permeability tests conducted over 24, 48, 72, and 96 hours were plotted against the values of compressive strength tests conducted at 1, 2, 3, and 4 days following 90 days of exposure.

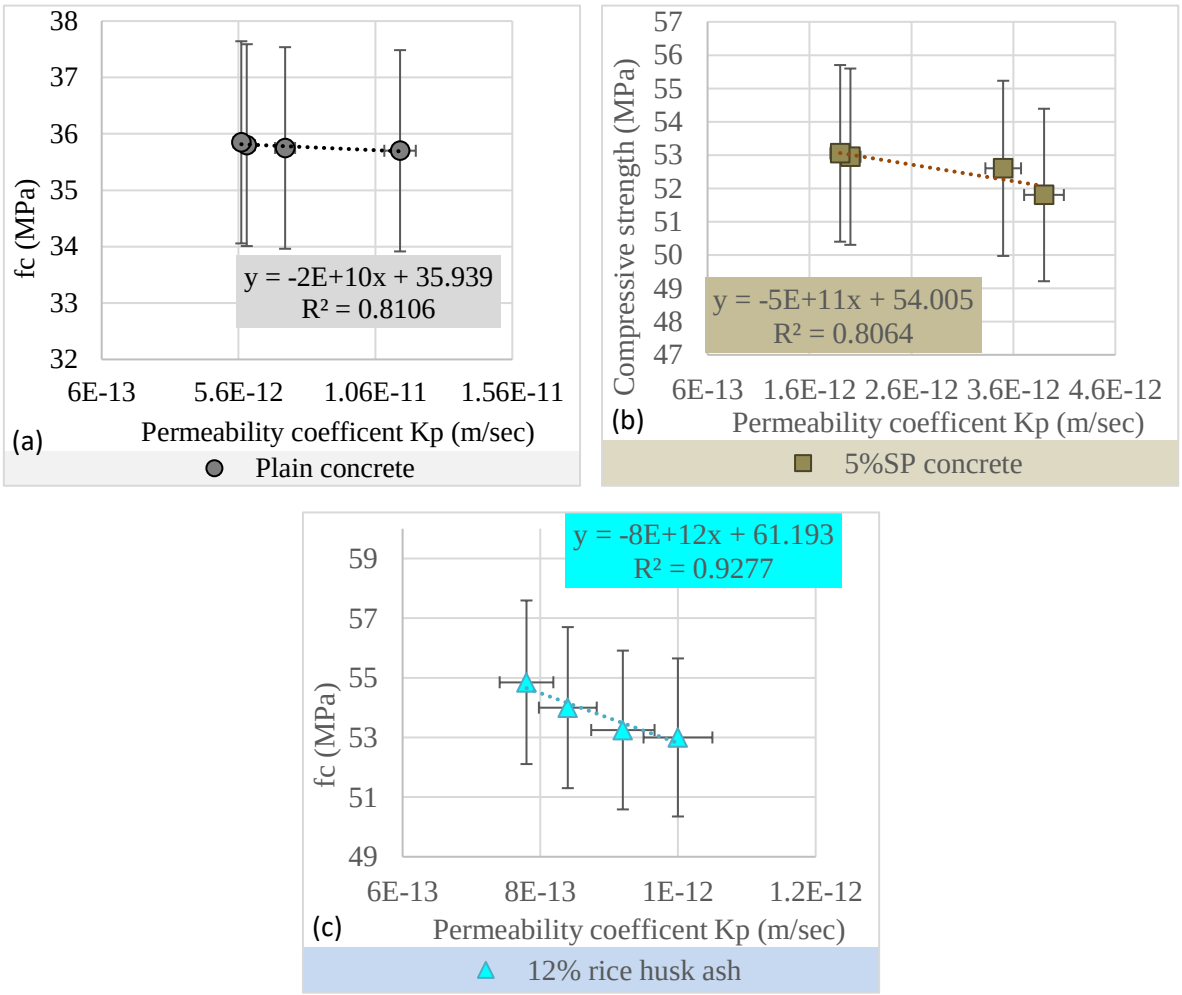

Fig. 16. Compressive strength versus permeability coefficient for: (a) P; (b) 5%SP; (c) 12%RHA concretes with 10mm maximum aggregate size.

It is evident that, for concrete with a maximum aggregate size of 10 mm, there is a strong association between strength growth and the decrease in permeability with an increase in test duration. The 12%RHA concrete generally exhibited the best resilience and the lowest permeability coefficient. The permeability of concrete plays a significant role in the corrosion of steel in concrete exposed to

harsh conditions, as water, oxygen, carbon dioxide, and chloride ions are the main agents in the corrosion process. Reducing environmental pollution can be greatly aided by using appropriate cement substitutes [26], which include silica fume, fly ash, slag and RHA [27]. The addition of finer (as opposed to larger) RHA particles limits the chloride ion penetration over time and improves the values for flexural, compressive, and tensile strength [28]. By adding agricultural waste, such as RHA, more sustainable concrete can be made [29]. A number of studies attempted to compare the performance of different types of cement substitutes such as silica fume and RHA [30]. Moreover, further use of superplasticizer-concrete in urban areas was studied [31]. Through the sustainable application of blended concrete, nano-materials and recycling materials [32] can support environmentally friendly construction practices [33]. Therefore, the goal of designers should be to create high-quality, dense concrete with limited permeability to prevent the entry of substances that cause corrosion.

4.5. Response surface plots

The Fig. 17 show a three-dimensional surface of response of compressive strength, graphical representations of the second order quadratic equation. It depicts the relationship between a response variable fc and two predictor variables: permeability coefficient and exposure period for plain concrete, Fig. (17a) and 12%RHA concrete, Fig. (17b).

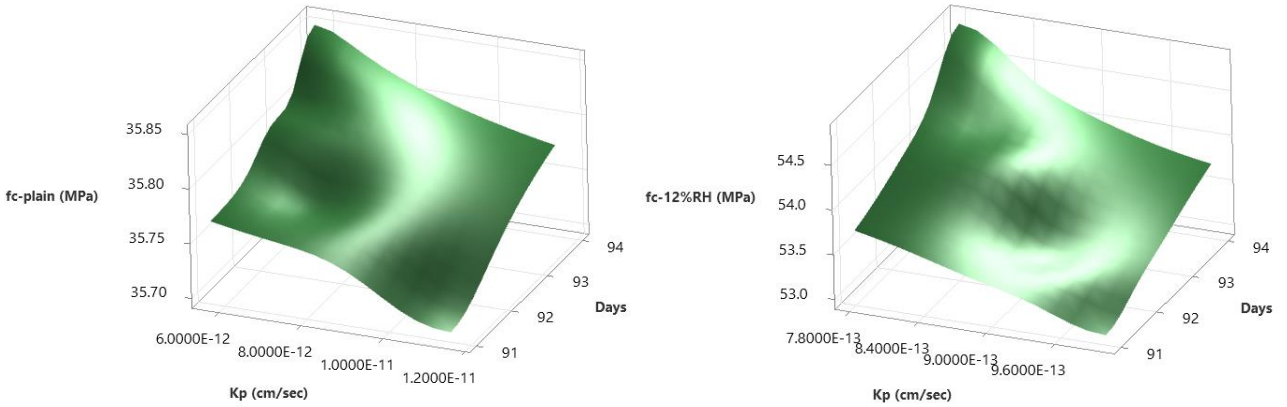

Fig. 17. 3D response surface plots Kp versus exposure period for compressive strength of 12%RHA concrete.

4.6. Statics

The strength of blended and plain concrete is affected by variations in various types of concrete. To assess the effect of maximum aggregate size and concrete type on the values of compressive strength, tensile splitting strength and flexural strength a 2-way analysis of variance (ANOVA) with replication was conducted. Table 3 shows the summary of the analysis conducted. As the value of $F_{statistic}$ is greater than $F_{critical}$, for the three cases. The statistical analysis indicate that the two different aggregate sizes, 10mm and 20mm, produced mean strengths that were statistically similar for the three different types of concrete specimens. Moreover, there was no overall pattern between the mixes with maximum aggregate sizes of 10 mm and 20 mm. Because the strengths of the various types of specimens were similar, it was not possible to identify any overall trends from the data.

Table 3. Summary of two-way ANOVA test with replication for strength.

Parameter	Variable	FStatistic	FCritical	P-value	α-value	Is FStatistic > FCritical	Is P value > α-value
MAS10	fc	91.95	2.60			Yes	
	ft	6.1	2.60			Yes	
	fr	36.48	2.60			Yes	
MAS20	fc	91.95	2.60	0.000034	0.05		Yes
	ft	6.1	2.60	0.00062	0.05		Yes
	fr	36.48	2.60	0.000	0.05		Yes

5. Conclusions

The current study examined the performance of one of the most widely used material in our world, concrete, incorporating chemicals (super-plasticizer) and mineral admixtures (12%RHA) under aggressive environments. Based on the experimental results from this research work, the following conclusions can be drawn:

- The compressive strength of plain concrete increased up to 6 months. Afterwards, the strength decreased slightly.
- There was a good compatibility between the superplasticizer and Portland cement. The use of superplasticizer increased compressive strength and enhanced the splitting and flexural tensile strengths of concrete.
- Concrete specimens containing 12% highly active RHA as a partial replacement by weight of cement showed superior strength performance over the other concretes by 10 to 30%.
- 12%RHA concrete specimens exhibit superior performance with an average reduction of 88% and 66% in the permeability values compared with plane and 5%SP concretes.
- Most of existing models for predicting tensile splitting and flexural strengths perform rather conservatively. The prosed models supersede the performance of existing models.
- The statistical analysis demonstrates that the compressive strength, splitting strength, and flexural strength were not significantly impacted by the variation in maximum aggregate size.

Potential future research directions include exploring different RHA sources, varying environmental conditions, or long-term performance assessments. This is in order to understand the effect of crushed aggregate, specimen size, presence of fibers, and two combined admixtures on various properties of a sustainable concrete when exposed to severe environmental conditions.

Funding

This research did not receive any specific grant from funding agencies in the public, commercial, or not-for-profit sectors.

Conflicts of interest

The authors declare that they have no known competing financial interests or personal relationships that could have appeared to influence the work reported in this paper.

Authors contribution statement

Nwzad Abduljabar Abdulla: The primary Investigation; Methodology; Software; Validation; review & editing manuscript text and formal analysis were done by the author.

References

[1] Mehta PK. "Durability of concrete in marine environment--A review. " Spec Publ n.d.;65:1-20.

[2] Xu XF, Wei CL, Zhang F. Concrete Random Damage Prediction Model under Seawater Chemical Erosion Environment. Appl Mech Mater 2011;90–93:857–61. https://doi.org/10.4028/www.scientific.net/AMM.90-93.857.

[3] Zhuang Z, Mu S, Guo Z, Liu G, Zhang J, Miao C. Diffusion-reaction models for concrete exposed to chloride-sulfate attack based on porosity and water saturation. Cem Concr Compos 2024;146:105378. https://doi.org/10.1016/j.cemconcomp.2023.105378.

[4] Aye T, Oguchi CT. Resistance of plain and blended cement mortars exposed to severe sulfate attacks. Constr Build Mater 2011;25:2988–96. https://doi.org/10.1016/j.conbuildmat.2010.11.106.

[5] Zhao G, Li J, Shi M, Cui J, Xie F. Degradation of cast-in-situ concrete subjected to sulphate-chloride combined attack. Constr Build Mater 2020;241:117995. https://doi.org/10.1016/j.conbuildmat.2019.117995.

[6] Carette VMM and GG. An Efficient Material.-Silica Fume Concrete - Properties, Applications, and Limitations. Concr Int 1983;5:40–6.

[7] Swamy RN. Cement replacement materials. Surrey Univ 1986;3.

[8] Ganesan K, Rajagopal K, Thangavel K. Rice husk ash blended cement: Assessment of optimal level of replacement for strength and permeability properties of concrete. Constr Build Mater 2008;22:1675–83. https://doi.org/10.1016/j.conbuildmat.2007.06.011.

[9] Ozturk E, Ince C, Derogar S, Ball R. Factors affecting the CO2 emissions, cost efficiency and eco-strength efficiency of concrete containing rice husk ash: A database study. Constr Build Mater 2022;326:126905. https://doi.org/10.1016/j.conbuildmat.2022.126905.

[10] Abduljabar Abdulla N. Strength models for uPVC-confined concrete. Constr Build Mater 2021;310:125070. https://doi.org/10.1016/j.conbuildmat.2021.125070.

[11] Al-Amoudi, Omar Saeed Baghabra, Mohammed Maslehuddin and AIA-M. Prediction of Long-Term Corrosion Resistance of Plain and Blended Cement concretes. ACI Mater J 1993;90. https://doi.org/10.14359/4430.

[12] Sahoo S, Parhi PK, Chandra Panda B. Durability properties of concrete with silica fume and rice husk ash. Clean Eng Technol 2021;2:100067. https://doi.org/10.1016/j.clet.2021.100067.

[13] EC2. Design of concrete structures: Part 1–1: General rules and rules for buildings, (2004). 2004.

[14] JCI-08 2008. Guideline for control of cracking of mass concrete, 2008.

[15] ACI 318–11. ACI 318–11, Building code requirements for structural concrete and commentary, 2011.

[16] Oluokun F. Prediction of Concrete Tensile Strength from its Compressive Strength: an Evaluation of Existing Relations for Normal Weight Concrete. ACI Mater J 1991;88. https://doi.org/10.14359/1942.

[17] Smadi M, Migdady E. Properties of high strength tuff lightweight aggregate concrete. Cem Concr Compos 1991;13:129–35. https://doi.org/10.1016/0958-9465(91)90008-6.

[18] Gesoğlu M, Özturan T, Güneyisi E. Shrinkage cracking of lightweight concrete made with cold-bonded fly ash aggregates. Cem Concr Res 2004;34:1121–30. https://doi.org/10.1016/j.cemconres.2003.11.024.

[19] Saradhi Babu D, Ganesh Babu K, Wee TH. Properties of lightweight expanded polystyrene aggregate concretes containing fly ash. Cem Concr Res 2005;35:1218–23. https://doi.org/10.1016/j.cemconres.2004.11.015.

[20] Meraz MM, Mim NJ, Mehedi MT, Noroozinejad Farsangi E, Arafin SAK, Shrestha RK, et al. On the utilization of rice husk ash in high-performance fiber reinforced concrete (HPFRC) to reduce silica fume content. Constr Build Mater 2023;369:130576. https://doi.org/10.1016/j.conbuildmat.2023.130576.

[21] AS 3600–18 2018. Australian standard for concrete structures, 2018.

[22] Rashno AR, Adlparvar M, Izadinia M. Study on Rheology Properties, Durability and Microstructure of UHPSCC Contains Garnet, Basalt, and Pozzolan. J Rehabil Civ Eng 2023;11:96–110.

https://doi.org/10.22075/JRCE.2022.25651.1584.

[23] Imad A. Khalhen 1 Reza Aghayari. Impact Resistance of Concrete Containing LLDPE–Waste Tire Rubber and Silica Fume. J Rehabil Civ Eng 2023;1:60–75. https://doi.org/10.22075/jrce.2022.23456.1511.

[24] Hossain KMA, Anwar MS. Performance of rice husk ash blended cement concretes subjected to sulfate environment. Mag Concr Res 2014;66:1237–49. https://doi.org/10.1680/macr.14.00108.

[25] Chindaprasirt P, Homwuttiwong S, Jaturapitakkul C. Strength and water permeability of concrete containing palm oil fuel ash and rice husk–bark ash. Constr Build Mater 2007;21:1492–9. https://doi.org/10.1016/j.conbuildmat.2006.06.015.

[26] Masoud Dadkhah 1 Ali Bandani 2 Reza Rahgozar 3 Peyman Rahgozar 4. Mechanical properties of self-compacting lightweight concrete containing pumice and metakaolin. J Rehabil Civ Eng 2024;12:97–118. https://doi.org/10.22075/jrce.2023.29150.1762.

[27] Abduljabar Abdulla N. Effect of saline environment on the strength of reinforced concrete beams. Al-Rafidain Eng J (AREJ) n.d.;28;1-23.

[28] Al-Alwan AAK, Al-Bazoon M, I.Mussa F, Alalwan HA, Hatem Shadhar M, Mohammed MM, et al. The impact of using rice husk ash as a replacement material in concrete: An experimental study. J King Saud Univ - Eng Sci 2024;36:249–55. https://doi.org/10.1016/j.jksues.2022.03.002.

[29] Pradhan SS, Mishra U, Biswal SK, Pramanik S, Jangra P, Aslani F. Effects of rice husk ash on strength and durability performance of slag-based alkali-activated concrete. Struct Concr 2024;25:2839–54. https://doi.org/10.1002/suco.202300173.

[30] Das SK, Singh SK, Mishra J, Mustakim SM. Effect of Rice Husk Ash and Silica Fume as Strength-Enhancing Materials on Properties of Modern Concrete—A Comprehensive Review, 2020, p. 253–66. https://doi.org/10.1007/978-981-15-1404-3_21.

[31] Teymouri E, Wong KS, Tan YY, Pauzi NNM. Mechanical behaviour of adsorbent pervious concrete using iron slag and zeolite as coarse aggregates. Constr Build Mater 2023;388:131720. https://doi.org/10.1016/j.conbuildmat.2023.131720.

[32] K. Srinivasan, S. Vivek, V. Sampathkumar. Facilitating Eco-Friendly Construction Practices with the Sustainable Application of Nanomaterials in Concrete Composites. J Environ Nanotechnol 2024;13:201–7. https://doi.org/10.13074/jent.2024.06.242556.

[33] Krishnaswami N, Velusamy S, Palanisamy C, Govindharajan G, Elanchezhiyan G, Ravi G. Experimental studies on recycled E-waste by using coarse aggregate in concrete. Mater Today Proc 2022;65:1996–2002. https://doi.org/10.1016/j.matpr.2022.05.328.